

PROCEEDINGS OF SPIE

[SPIDigitalLibrary.org/conference-proceedings-of-spie](https://spiedigitallibrary.org/conference-proceedings-of-spie)

Systematic measurements of the aerosol extinction-to-backscatter ratio

Gelsomina Pappalardo, Aldo Amodeo, Lucia Mona, Marco Pandolfi

Gelsomina Pappalardo, Aldo Amodeo, Lucia Mona, Marco Pandolfi, "Systematic measurements of the aerosol extinction-to-backscatter ratio," Proc. SPIE 5653, Lidar Remote Sensing for Industry and Environmental Monitoring V, (12 January 2005); doi: 10.1117/12.578809

SPIE.

Event: Fourth International Asia-Pacific Environmental Remote Sensing Symposium 2004: Remote Sensing of the Atmosphere, Ocean, Environment, and Space, 2004, Honolulu, Hawai'i, United States

Systematic measurements of the aerosol extinction-to-backscatter ratio

G. Pappalardo*, A. Amodeo, L. Mona, M. Pandolfi

Istituto di Metodologie per l'Analisi Ambientale IMAA – CNR
C.da S. Loja, Tito Scalo, Potenza, Italy I-85050

ABSTRACT

Systematic lidar measurements of aerosol backscatter and extinction in the troposphere were performed since May 2000 with the aerosol lidar system operational at IMAA-CNR in Tito Scalo (Potenza) (Southern Italy, 40°36'N, 15°44'E, 820 m above sea level) in the framework of EARLINET. EARLINET is the first European network of 22 advanced lidar stations operating to provide a quantitative climatological database of the horizontal, vertical and temporal distribution of aerosols over Europe. Aerosol backscatter measurements were performed at both 355 nm and 532 nm, while aerosol extinction coefficient was retrieved from simultaneous N₂ Raman backscatter signals at 386.6 nm. The lidar measurements at IMAA have been performed according to a regular schedule of two night time measurements per week (around sunset) and one daytime measurement per week (around 13:00 UT). Further measurements were devoted to observe special events such as Saharan dust, forest fires and volcanic eruptions. A statistical analysis on climatological aerosol extinction-to-backscatter ratio (lidar ratio) data, covering more than three years of systematic lidar observations, has been carried out. These lidar ratio data, in conjunction with an analysis on the air masses backtrajectories, provide information on microphysical properties of the aerosol on a wide range of meteorological conditions. Results obtained starting from both climatological data and special events (Saharan dust and volcanic eruptions) are presented and discussed.

Keywords: Lidar, aerosol, Raman, EARLINET, networking

1. INTRODUCTION

Atmospheric aerosols represent one of the largest source of uncertainty in the predictions of the future global climate¹, mainly as a consequence of their high unhomogeneity and variability both in space and in time^{2,3}. The determination of the aerosol effects on the Earth's radiative balance is complicated by the presence of many different aerosol sources, like deserts, forest fires, sea spray and volcanoes generating aerosols in the atmosphere with very variable concentration, size distribution, composition, chemical and physical properties.

The tropospheric aerosols are mainly concentrated within the Planetary Boundary Layer (PBL), the lowest part of the atmosphere directly influenced by the Earth's surface. As a consequence of the strong convective activity, like during Saharan dust outbreaks or during volcanic eruptions episodes, the aerosols are directly injected into the troposphere and transported over long distances from their source region^{4,5}. The Sahara regions, for example, are considered as a major sources of mineral dust with billions tons transported every years worldwide⁶.

In order to reduce the uncertainty related to the aerosol effect on climate, sporadic in situ measurements are not sufficient mainly because of the high variable aerosol composition and concentration. It is recognized that this degree of uncertainty can be reduced only with a climatological analysis based on high accuracy aerosol measurements carried out with continuity and on long time period.

Lidars represent a very powerful optical remote sensing technique because they are able to provide information on several atmospheric parameters with very high spatial and temporal resolutions, important requirement for the parameterisations of the climate model and for the development of global chemistry. Lidar techniques are necessary

*pappalardo@imaa.cnr.it; phone +39 0971427265; fax +39 0971427271

because they allow to characterise atmospheric aerosols in terms of spatial behaviour of extinction and backscatter coefficients, lidar ratio, optical depth and microphysical properties such as shape, refractive index and size distribution^{7,8}. The increasing interest of the scientific community in lidar applications for atmospheric studies is attested by the tendency to establish lidar networks at continental scale in order to improve the knowledge of the aerosol effects on climate. At present, at European scale it is operational the first aerosol lidar network, established in the frame of the EARLINET project (European Aerosol Research Lidar NETwork), of which the IMAA tropospheric lidar system is part^{9,10,11}. Starting on May 2000 the EARLINET lidar network has been created with the main objective to establish a qualitatively and quantitatively significant database for the horizontal and vertical distributions of atmospheric aerosol over Europe¹². Up to now, at IMAA, Potenza – South Italy (40°36'N-15°44'E, 820 m a.s.l.), more than 2000 hours of measurements have been collected with the tropospheric aerosol lidar system. These measurements can be subdivided in two main categories: regular measurements, systematically performed three times a week both in night time and in daytime conditions, and special measurements, related to special events like Saharan dust outbreaks⁵, volcanic eruptions⁴, large forest fires and so on. In this paper, we present a statistical analysis of the lidar ratio measurements within the Planetary Boundary Layer, starting from the systematic observations. Lidar ratio measurements related to Saharan dust outbreaks and volcanic eruptions will be also discussed.

2. TROPOSPHERIC AEROSOL EXTINCTION-TO-BACKSCATTER RATIO MEASUREMENTS

The tropospheric aerosol lidar system operational at IMAA is based on a Nd:YAG laser, with a repetition rate up to 20 Hz¹⁰. The second (532 nm) and the third (355 nm) harmonics are transmitted in atmosphere in a coaxial mode. The backscattered radiation is collected by means of a vertically pointing telescope in Cassegrain configuration with a 0.5 m diameter primary mirror and a combined focal length of 5 m. The collected radiation is split into three channels by means of dichroic mirrors, and interferential filters with a bandwidth of 1 nm are used to select the elastic backscattered radiation at 532 nm and 355 nm, and the N₂ Raman shifted signals at 386.6 nm. Acquisition is performed both in analogical and photon counting mode.

With this system it is possible to perform independent measurements of aerosol extinction and backscatter coefficient in the UV region, consequently it is possible to retrieve the extinction-to-backscatter ratio (lidar ratio), vertical profiles¹³. This parameter links two optical parameters both depending on the laser wavelength and on the size distribution, shape and chemical composition of the atmospheric aerosols and consequently lidar ratio measurements allow to retrieve information about microphysical properties of the aerosols^{14,15}.

The statistical analysis reported in the next section is based on three years of systematic aerosol lidar measurements performed at IMAA and is performed within the PBL the depth of which, that is its height, represents a critical parameter also in the physicochemical and dynamic processes occurring in the lower atmosphere.

The aerosols are usually used as tracers for the study of the boundary layer vertical structure and dynamics and different methods can be used to determine the PBL height by lidar¹⁶⁻²⁰. Starting from the statement that the optical power received by lidar is proportional to the atmospheric aerosol content, the method we used consists in performing the first-order derivative of averaged range corrected lidar signals (RCLS) $z^2 P_{\lambda_e}(z)$ [$\partial RCLS / \partial z$] looking for its significant minimum, this latter corresponding to a strong gradient in the range corrected lidar signal and consequently to the boundary between the free troposphere and the Planetary Boundary Layer.

An example of PBL height determination by lidar is showed in figure 1a, where the range corrected lidar signal at 355 nm (open circles), measured at IMAA on May 13, 2003, and its first-order derivative (solid circles) as a function of height are reported. The range corrected signal showed has a vertical resolution of 60 m and was obtained by integrating 10 lidar profiles (from 21:05 UT to 21:15 UT) each of which was acquired with an integration time of 1 min and a vertical resolution of 15 m.

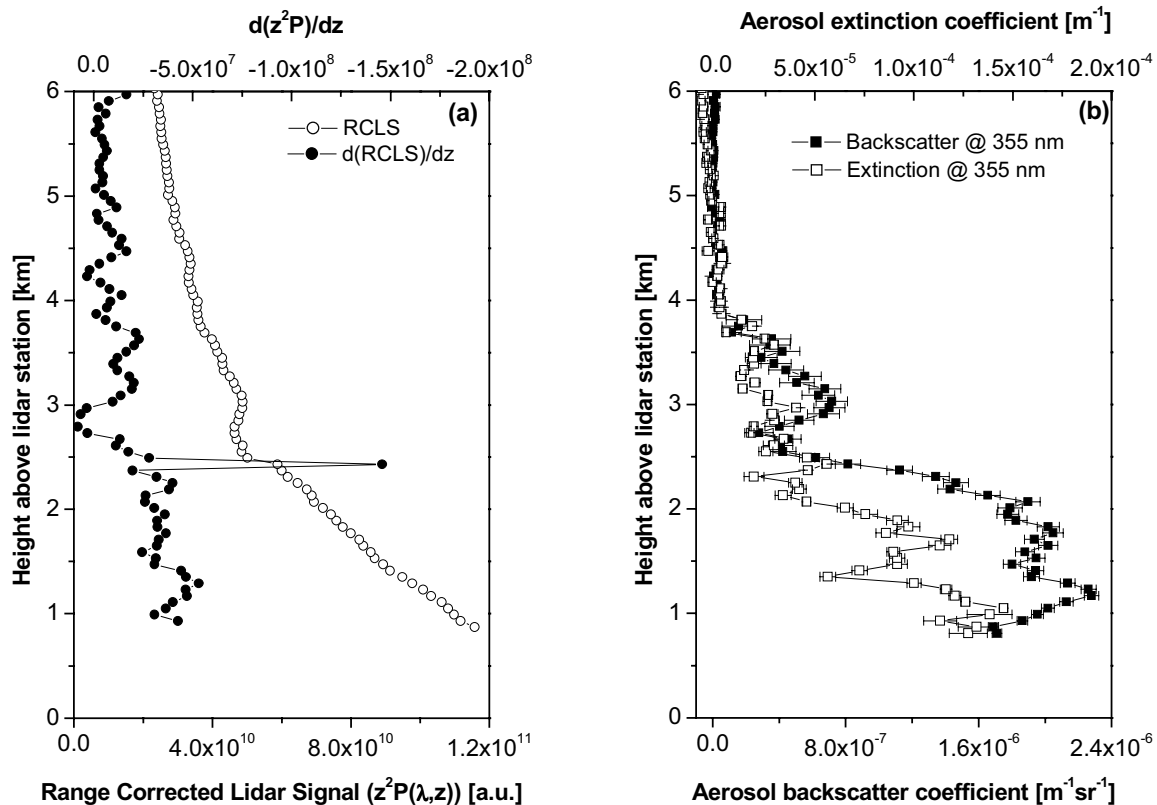


Figure 1: (a) Range corrected lidar signal at 355 nm (open circles) and its first-order derivative (solid circles). (b) Aerosol backscatter (solid squares) and aerosol extinction (open squares) profiles at 355 nm [IMAA, May 13, 2003 (21:05-21:15 UT)].

The first-order derivative in figure 1a shows an evident minimum around 2400 m of height above lidar station due to a gradient in the range corrected lidar signal and corresponding to the height of the PBL. In figure 1b, the aerosol backscatter coefficient and the extinction coefficient profiles at 355 nm provided by lidar for the same measurement of May 13, 2003 are also reported. As for the range corrected signal, the aerosol extinction and backscatter profiles have been obtained by integrating lidar signals from 21:05 UT to 21:15 UT. The effective resolution of the extinction profile is 180 m up to 2.4 km of height above lidar station, 240 m from 2.4 km up to 4 km and 320 m up to 6 km while the resolution of the aerosol backscatter coefficient profile is 60 m for each height range. As shown in figure 1b, most of the aerosol load is contained within the PBL, below 2400 m of height above lidar station, with values of aerosol backscatter coefficient ranging from $8 \times 10^{-7} m^{-1}sr^{-1}$ to $2.3 \times 10^{-6} m^{-1}sr^{-1}$, and with aerosol extinction values ranging between $1.9 \times 10^{-5} m^{-1}$ and $1.5 \times 10^{-4} m^{-1}$. Typical errors are below 5% and 10% within the PBL for the aerosol backscatter and extinction coefficient respectively.

In figure 2, the lidar ratio profile at 355 nm obtained from the ratio between the aerosol extinction and backscatter coefficients showed in figure 1b is reported. Lidar ratio values present a large variability as a function of the altitude as a consequence of the high variability in the size and/or microphysical properties of the aerosol. These values can be observed in the profile in figure 2 ranging between 21 sr and 78 sr within the PBL with a mean value of 44 ± 16 sr. This value, as we will see in the next section, is very close to the mean lidar ratio value calculated within the PBL on three years of systematic aerosol lidar measurements.

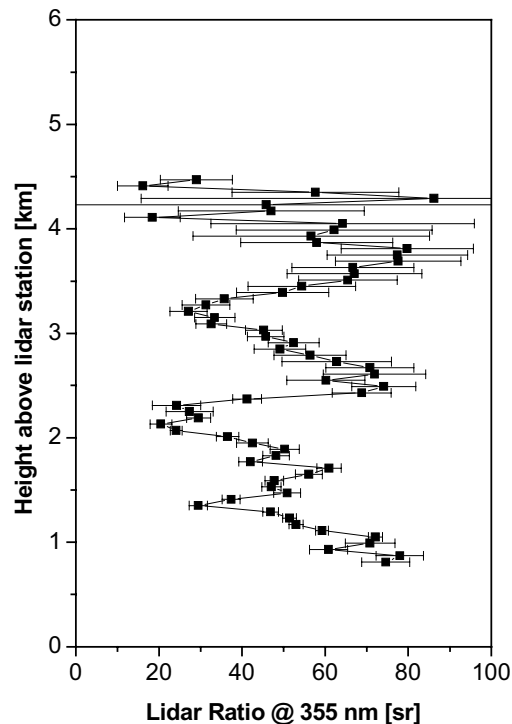


Figure 2: Lidar ratio vertical profile at 355 nm measured at IMAA on May 13, 2003 (21:05-21:15 UT).

3. LIDAR RATIO STATISTICAL ANALYSIS

Starting from May 2000, regular lidar measurements of aerosol extinction and backscatter are performed in Potenza three times a week. These data collected with the IMAA lidar system allow to perform a statistical analysis of the aerosol typically present over our site. The analysis reported in this paper has been performed within the PBL in terms of aerosol optical depth and mean lidar ratio values at 355 nm. The analysis is based on a set of data covering with continuity and homogeneity a temporal period of more than three years since May 2000 and only the regular after-sunset measurements obtained on cloud-free conditions are considered, for a total of about 100 vertical profiles.

The aerosol optical depths have been obtained starting from the aerosol extinction vertical profiles by extrapolating the lowest data point down to the ground, that is assuming constant values of the extinction in this lowest layer, typically the first 800 m above the lidar station. This assumption may result in large errors if the boundary layer is not well mixed but this condition is usually verified at the sunset.

Figure 3 shows the PBL heights above the lidar station (figure 3a), the aerosol optical depth (figure 3b) and the mean lidar ratio values (figure 3c) calculated within the PBL as a function of the day of the year.

The annual behaviors of PBL height and aerosol optical depth show a clear seasonal dependence, as evidenced by the six-weeks sliding averages reported in the figures.

The seasonal dependence of the PBL height is closely related to the solar heating of the Earth's surface during the year, being this latter higher in the summer period and lower in the winter one. The six-weeks sliding average, reported in the figure 3a, shows a very evident seasonal dependence of the PBL height with the highest values observed in the period May-July with values around 1600-1750 m, while the lowest values, around 1200 m, are observed in the period between the end of December and January. A larger variability in the PBL height has been observed in the summer periods when PBL heights higher than 2000 m or lower than 1300 m are quite frequently observed.

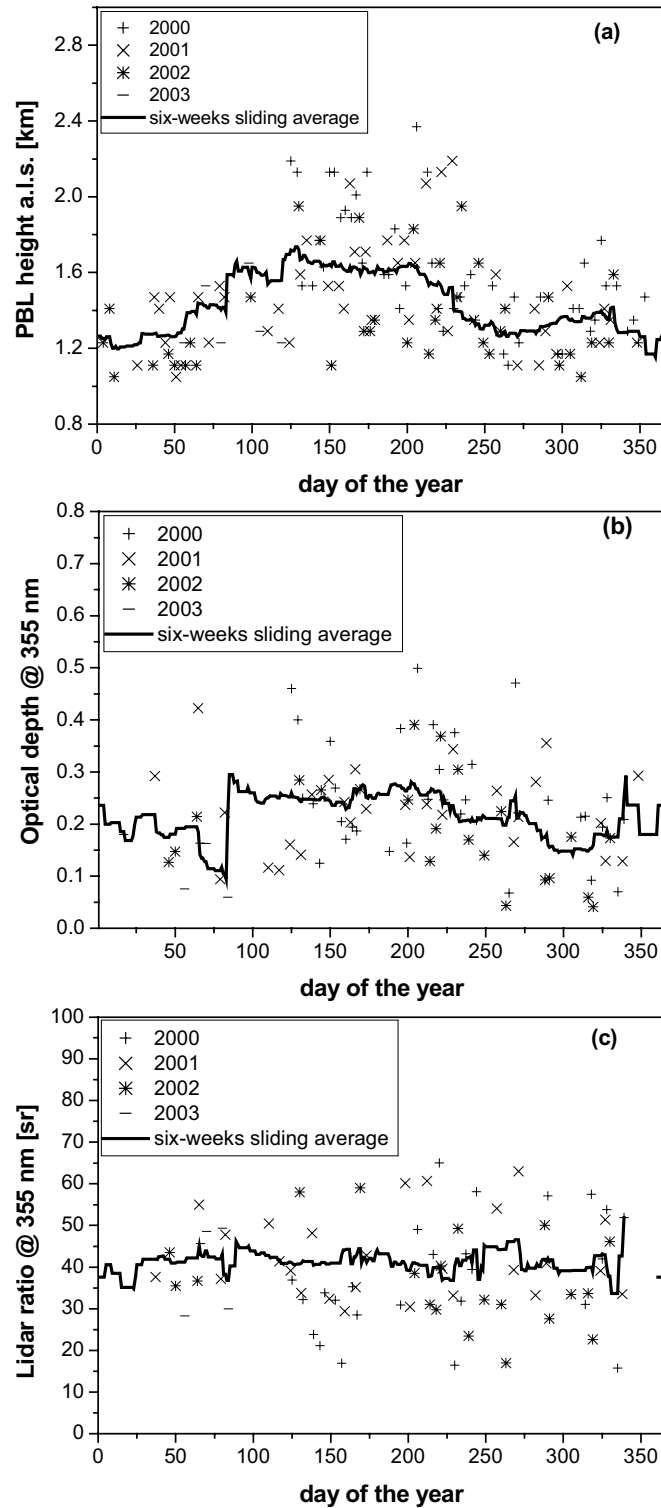


Figure 3: Annual cycle of the Planetary Boundary Layer height above the IMAA lidar station (a), of the optical depth at 355 nm (b) and of the mean lidar ratio values (c). The solid lines represent the six-weeks sliding averages. Symbols +, x, * and —, refer to the measurements performed on 2000, 2001, 2002 and 2003 respectively.

A strong seasonal dependence can be observed also for the aerosol optical depth calculated within the PBL. As evidenced in figure 3b, it presents large fluctuations of their values during the year demonstrating the large variability of the aerosol load. Typically, the highest values are observed only during the summer periods, while lower values are observed both in winter and in summer, this resulting in a very pronounced seasonal dependence of this parameter, and this variability is related not only to the higher aerosol load in the summer period respect to the winter period, but also to the variability of the PBL height where the aerosol optical depths have been calculated.

These considerations are quite different in the case of the lidar ratio. Each lidar ratio value reported in figure 3c is calculated by averaging the values of the lidar ratio vertical profile within the PBL. In contrast with the aerosol optical depth, which is higher in summer and lower in winter, the lidar ratio measurements do not show appreciable differences between winter and summer periods, as evidenced by the six-weeks sliding average reported in figure 3c. For the summer and winter periods, the lidar ratio mean values, reported in table 1, are 38.4 sr and 41.0 sr with standard deviations of 12.8 sr and 10.6 sr respectively, very close to 39.4 sr, the mean value calculated for the whole period considered in this analysis (May 2000-April 2003).

Table 1: Lidar ratio mean values calculated within the PBL, for the period May 2000-April 2003 and for the summer and winter period separately.

<i>Lidar ratio @ 355 nm</i>		
category	mean [sr]	st. deviation [sr]
May 2000 – April 2003	39.4	11.8
summer	38.4	12.8
winter	41.0	10.6

Average lidar ratio values range from a minimum of 15.7 sr to a maximum of 57.5 sr for winter periods and from 16.4 sr to 65.0 sr for summer periods. There is a difference between the annual cycle of the optical depth and the lidar ratio: in the case of the lidar ratio higher values can be observed in winter period as well as in the summer period. This is because lidar ratio does not depend on the aerosol load or on the PBL height as for the optical depth, but it is strongly related to the microphysical properties of aerosol, which can rapidly change from day to day as evidenced by the lidar ratio values reported in figure 3c and this obviously depends on the history of the air mass transported to the measurement site. The air mass origin and transport has been investigated by using the 96h-backtrajectories analysis provided by the German Weather Service. Considering the typical advection patterns for the air masses ending within the PBL over our site, 4 classes have been selected and reported in figure 4: the *Mediterranean Sea* class (figure 4a), with backtrajectories originating and remaining over the Mediterranean Sea, the *West* class (figure 4b) with backtrajectories originating in western Europe and ending over our site crossing through the Mediterranean Sea area, the *South* class (figure 4c), with backtrajectories originating over the Sahara region, and the *North* class (figure 4d), where both slow and fast air masses coming from the continent have been considered. The German Weather Service provides the 96h-backtrajectories analysis twice a day (13:00 and 19:00 UT) and for six different arrival levels over the measurement site (975, 850, 700, 500, 300, 200 hPa) as reported in figure 4. We are interested to study aerosol properties in well mixed conditions of the Planetary Boundary Layer and therefore we considered in our analysis only the 850 hPa and the 700 hPa backtrajectories and only those generated at 19:00 UT.

Figure 5 shows the mean lidar ratio values and aerosol optical depth calculated within the PBL, divided in the 4 air mass classes considered and the error bars reported in the figure indicate the standard deviation of the data. The lowest values for both lidar ratio and aerosol optical depth have been observed for the *Mediterranean Sea* class where mainly maritime aerosols are present, while the highest values have been observed for the North class related to continental and more polluted aerosols.

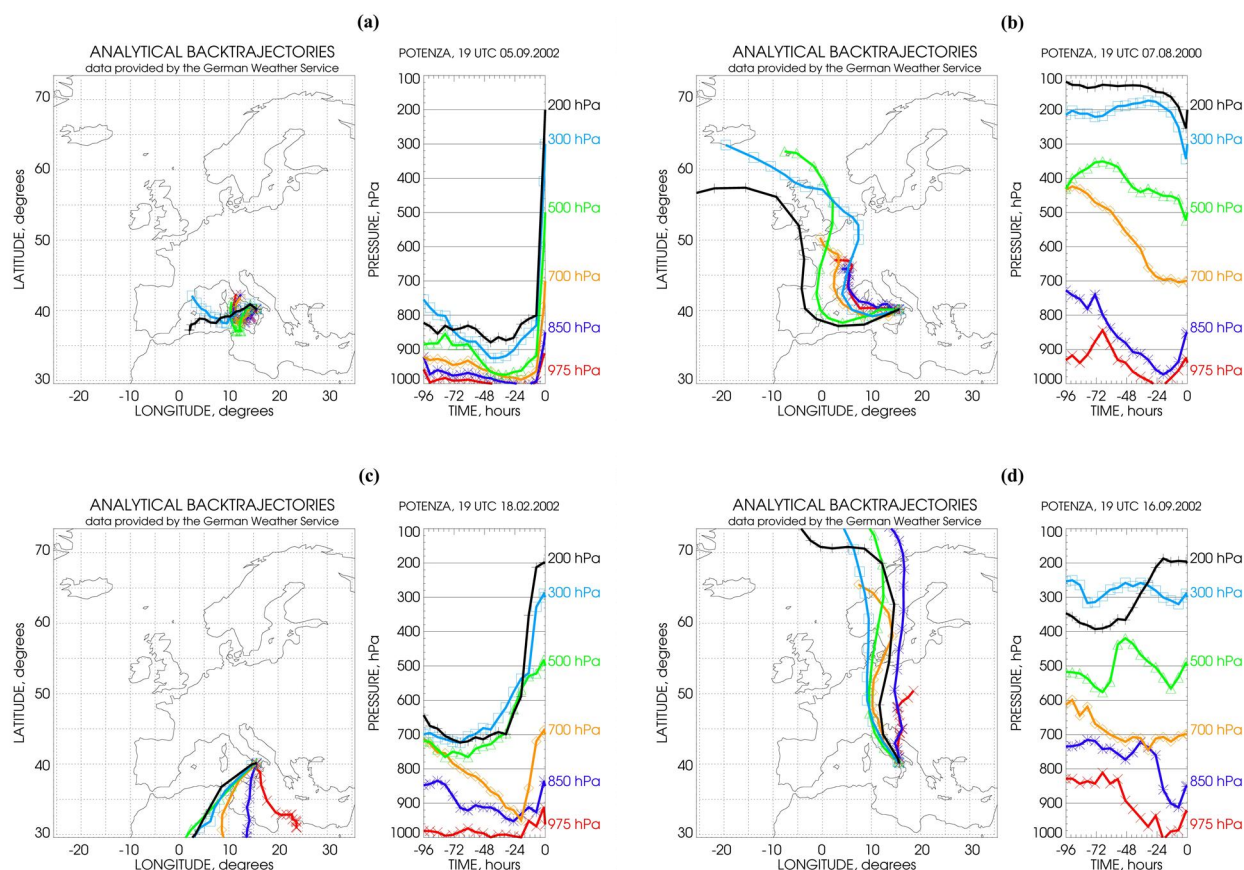


Figure 4: Typical advection patterns for the air masses ending within the Planetary Boundary Layer over Potenza: (a) Mediterranean Sea class, (b) West class, (c) South class, (d) North class.

4. LIDAR RATIO IN THE CASE OF SPECIAL EVENTS

Starting from May 2000, in addition to the regular measurements performed within EARLINET three times a week, special measurements campaign are performed in order to study particular atmospheric events like Saharan dust intrusions, very often observed at the IMAA lidar station and volcanic eruptions.

More than 100 Saharan dust cases have been observed, mainly as a consequence of the relatively small distance from the dust sources. Most of these events have been observed in the period between May and July²¹, while in winter time the observed cases are less frequent depending on the seasonal behavior of the Saharan dust intrusion in the Mediterranean basin²². Typically, observed Saharan dust layers extend between 2.5 and 6 km above sea level, with a maximum altitude of about 8 km a.s.l. and intrusions in the PBL are also observed. The aerosol optical depth calculated in the Saharan dust layers is largely variable with values ranging between 0.001 and 0.4 at 355 nm and with a mean value of about 0.12 and a standard deviation of 0.09. This variability is related to the large natural variability of Saharan dust emission phenomena, the highly variable dust composition and the modification processes occurred during the transport. As a consequence, as evidenced in figure 6, the mean lidar ratio values calculated within the dust layers present a large variability, ranging between 6 and 78 sr with a mean values of 37 sr and standard deviation of 15 sr. However, the aerosol optical depth shows a seasonal behavior with a maximum mean value of 0.19, at the end of June, and a minimum mean value of 0.03, at the middle of November. For summer and winter periods the lidar ratio mean values are not significantly different, being 39 ± 17 sr the mean summer value and 32 ± 9 sr the mean winter value, but the summer values distribution is wider as well as the variability along the individual aerosol layers²¹.

Two Etna volcano (Sicily, South Italy, 37°44' N, 15° E) eruption events occurred in July 2001²¹ and November 2002⁴. Both these events have been studied with the IMAA lidar system and for the first time measurements of the lidar ratio for tropospheric volcanic aerosol have been performed.

In figure 7, the aerosol backscatter and extinction coefficients vertical profiles at 355 nm and the corresponding lidar ratio vertical profile, acquired during the Etna eruption in 2002 are reported. The measurement was performed on 1 November 2002 when a direct transport of the Etna plume over the IMAA lidar station was observed. The vertical resolution for the reported profiles is 180 m and the time integration is 30 min. between 23:20 and 23:50 UT. In figure 7 the Etna plume is well distinguishable between 4 and 4.5 km above sea level, with peak values of about $5.1 \times 10^{-6} \text{ m}^{-1} \text{ sr}^{-1}$ and $2.2 \times 10^{-4} \text{ m}^{-1}$ for the aerosol backscatter and extinction respectively, about 20 times higher compared to the background values measured at this altitude during three years of measurements considered in the statistical analysis previously reported. The lidar ratio vertical profile (figure 7b) shows two different atmospheric regions where the lidar ratio is almost constant: the first corresponding to the PBL, up to about 2.6 km a.s.l., with a mean lidar ratio of $30 \pm 1 \text{ sr}^{23}$, and the second between 4 and 4.5 km a.s.l. with a mean value of $55 \pm 4 \text{ sr}$. The high mean lidar ratio value measured in this upper layer is related to the presence of sulfate particles directly transported from the volcano⁴.

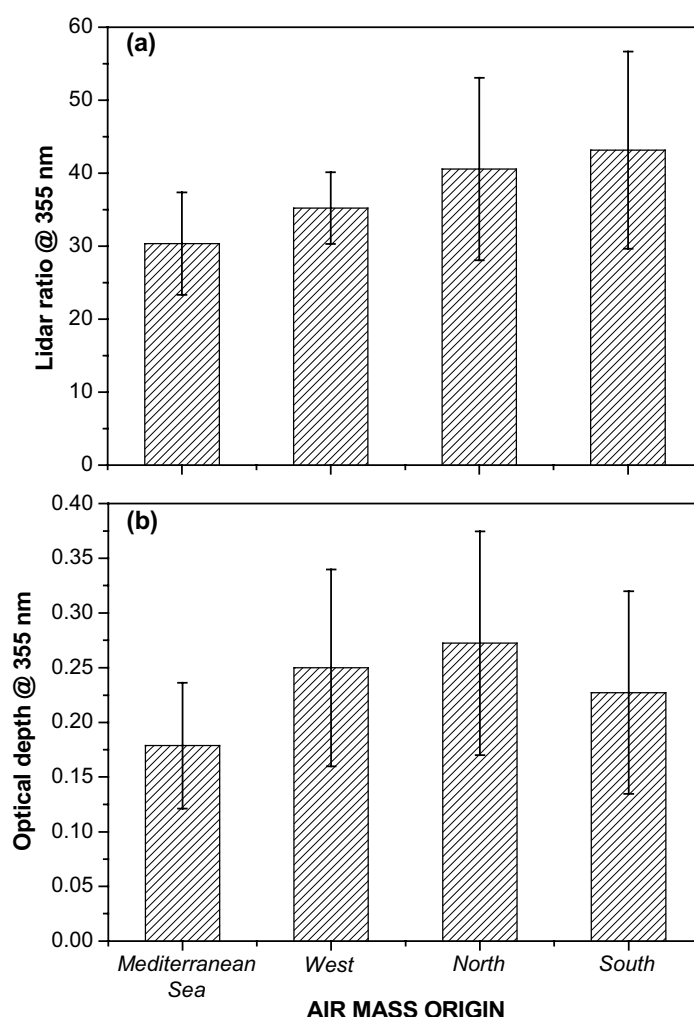


Figure 5: Mean lidar ratio values (a) and optical depth (b) at 355 nm calculated within the PBL, as a function of the air mass origin.

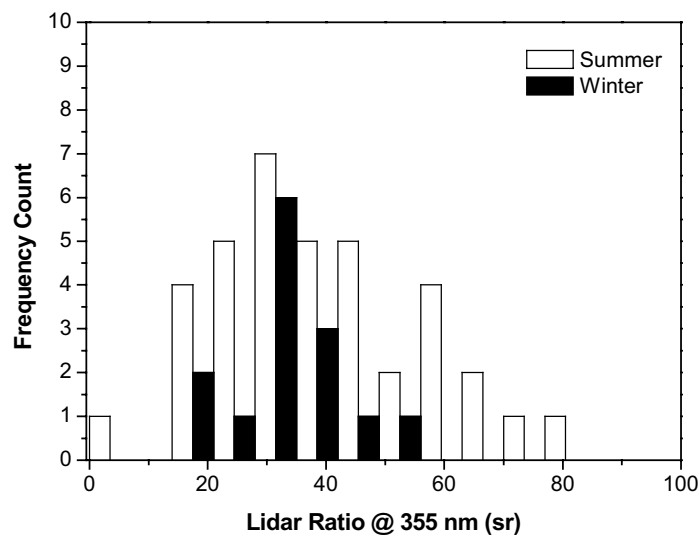


Figure 6: Frequency counts for the mean lidar ratio values measured within the Saharan dust layers for summer and winter periods (2000, 2001, 2002 and 2003) separately.

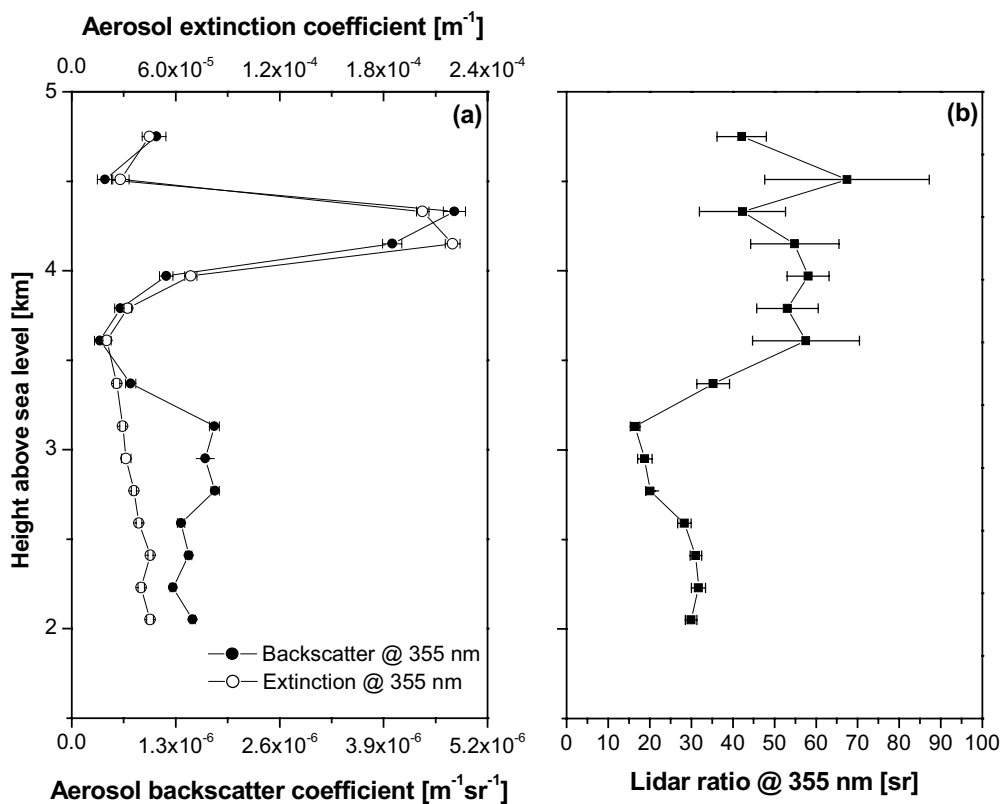


Figure 7: Aerosol backscatter and extinction coefficient vertical profiles at 355 nm (a) and lidar ratio vertical profile at 355 nm (b) measured on 1 November 2002, from 23:20 to 23:50 UT.

5. CONCLUSIONS

More than three years of systematic lidar measurements of aerosol backscatter and extinction in the troposphere, performed at IMAA, have been used for statistical study of the aerosol in the Planetary Boundary Layer.

In particular, the annual behavior and seasonal dependence of the height of the PBL and of the aerosol optical depth and of the mean lidar ratio within the PBL, have been presented and discussed. The aerosol optical depth shows a seasonal dependence with highest values in the period between April and September, with mean values around 0.26, respect to those measured in the winter period, when averaged values around 0.17 have been measured. This annual variability is in part related to the variability of the Planetary Boundary Layer height during the year. In fact, the PBL height is characterized by a high seasonal dependence, with values that in average vary between summer and winter. The highest PBL heights have been observed in the period May-July with values around 1600-1750 m above lidar station, while the lowest, around 1150-1250 m, in the period between the end of December and January. On the other side, the lidar ratio measurements do not show appreciable differences between winter and summer with mean values of 38.4 sr and 41.0 sr and standard deviations of 12.8 sr and 10.6 sr, respectively. These values are very close to 39.4 sr, the mean value calculated for the three years period of lidar measurements considered for the reported statistical analysis. An analysis of the observed lidar ratio values as a function of the air mass origin and transport has been performed. Lowest lidar ratio values have been observed for air masses originating over the Mediterranean Sea and obviously related to maritime aerosols while highest values have been observed for more polluted continental air masses.

Beside regular measurements, special measurements campaign have been performed in order to study particular atmospheric events like Saharan dust intrusions or volcanic eruption like those of the ETNA volcano. Since May 2000, more than 100 Saharan dust cases have been observed. Typical Saharan dust layers extend between 2.5 and 6 km above sea level with mean lidar ratio values, calculated within the dust layers, characterized by a large variability, ranging between 6 and 78 sr with a mean values of 37 sr and standard deviation of 15 sr.

During the 2002 Etna eruption a mean lidar ratio value of 55 ± 4 sr has been observed over the IMAA lidar station, typical of presence of sulfate particles directly transported from the volcano.

ACKNOWLEDGEMENT

The financial support of this work by the European Commission under grant EVR1-CT1999- 40003 is gratefully acknowledged.

The authors also thank the German Weather Service for the air mass backtrajectory analysis.

REFERENCES

1. IPCC Climate change 2001: the scientific basis, Cambridge University Press, Cambridge, UK, 881, PP, 2001.
2. Flowers E.C., McCormick R.A., and Kurfis K.R., Atmospheric turbidity over the United States, 1961-1966, *J. Appl. Meteorol.*, 8, 955- 962, 1969.
3. Twomey S., Pollution and the planetary albedo, *Atmos. Environ.*, 8, 1251-1256, 1974.
4. Pappalardo G., Amodeo A., Mona L., Pandolfi M., Pergola N., and Cuomo V., Raman lidar observations of aerosol emitted during the 2002 Etna eruption, *Geophys. Res. Lett.*, 31, 2004.
5. Mona L., Amodeo A., Pandolfi M., Pappalardo G., Three years of saharan dust observations over Potenza in the framework of EARLINET, Reviewed and Revised Papers presented at the 22nd International Laser Radar Conference, Gelsomina Pappalardo and Aldo Amodeo Editors, ESA SP-561, 849-852, 2004.
6. D'Almeida, G.A., A model for Saharan dust transport, *J. Clim. Appl. Meteorol.*, 24, 903-916, 1986.
7. Ferrare R. A., et al. Raman lidar measurements of aerosol extinction and backscattering 2. Derivation of aerosol real refractive index, single-scattering albedo, and humidification factor using Raman lidar and aircraft size distribution measurements, *J. Geophys. Res.*, Vol. 103, n. D16, 19,673-19,689, 1998.
8. Di Girolamo, P., Gagliardi, R.V., Pappalardo, G., Spinelli, N., Velotta, R., and Berardi, V., Two-wavelength lidar analysis of stratospheric aerosol size distribution, *J. Aerosol Sci.*, 26, N. 6, 989-1001, 1995.

9. Pappalardo, G. et al. Aerosol lidar intercomparison in the framework of the EARLINET project. 3 -Raman lidar algorithm for aerosol extinction, backscatter and lidar ratio, *Appl. Opt.*, Vol. 43, N. 28, 5370-5385, 2004.
10. Matthias, V. et al. Aerosol lidar intercomparison in the framework of the EARLINET project. 1 Instruments, *Appl. Opt.*, Vol. 43, N. 4, 961-976, 2004.
11. Matthias V., Balis D., Bösenberg J., Eixmann R., Iarlori M., Komguem L., Mattis I., Papayannis A., Pappalardo G., Perrone M. R., and Wang X., Vertical aerosol distribution over Europe: Statistical analysis of raman lidar data from 10 european Aerosol Research Lidar Network (EARLINET) stations, *J. Geophys. Res.*, Vol. 109, D18201, doi: 1029/2004JD004638, 2004.
12. Bösenberg J., et al. A European Aerosol Research Lidar Network to Establish an Aerosol Climatology, MPI-Report 348, Max-Planck-Institut für Meteorologie, Hamburg, 2003.
13. Ferrare R. A., et al. Raman lidar measurements of aerosol extinction and backscattering 2. Derivation of aerosol real refractive index, single-scattering albedo, and humidification factor using Raman lidar and aircraft size distribution measurements, *J. Geophys. Res.*, Vol. 103, n. D16, 19,673-19,689, 1998.
14. Ansmann A., Riebesell M., and Weitkamp C., Measurement of atmospheric aerosol extinction profiles with a Raman lidar, *Opt. Lett.* 15, 746–748, 1990.
15. Ansmann A., Wandinger U., Riebesell M., Weitkamp C., and Michaelis W., Independent measurement of extinction and backscatter profiles in cirrus-clouds by using a combined Raman elastic-backscatter lidar, *Appl. Opt.*, 31, 7113–7131, 1992.
16. Menut L., Flamant C., Pelon J., and Flamant P.H., Urban Boundary Layer Height determination from lidar measurements over the Paris Area, *Appl. Opt.*, 38, N. 6, 945, 1999.
17. Melfi S. H., Spinhirne, J. D., Chou S.-H., and Palm S. P., Lidar observations of the vertically organized convection in the planetary boundary layer over the ocean, *J. Climate Appl. Meteorol.*, 24, 806-821, 1985.
18. Flamant C., Pelon J., Flamant P. H., and Durand P., Lidar determination of the entrainment zone thickness at the top of the unstable marine atmospheric boundary-layer, *Boundary-Layer Meteorol.* 83, 247-284, 1997.
19. Hooper W. P., and Eloranta E., Lidar measurements of wind in the planetary boundary layer: the method, accuracy and results from joint measurements with radiosonde and kytoon, *J. Climate Appl. Meteorol.* 25, 990-1001, 1986.
20. Piironen A. K. And Eloranta E. W., Convective boundary layer mean depths and cloud geometrical properties obtained from volume imaging lidar data, *J. Geophys. Res.* 100, 25569-25576, 1995.
21. Mona L., A. Amodeo, M. Pandolfi, G. Pappalardo, Observation of Special Events at EARLINET Lidar Site of Potenza, in *Lidar Remote Sensing In Atmospheric and Earth Sciences*, pp. 361-364, 21th International Laser Radar Conference, Quebec City, Canada, 8-12 July, 2002
22. Prospero J.M., Long-range transport of mineral dust in the global atmosphere: Impact of African dust on the environment of the southeastern United States, *Proc. Natl. Acad. Sci. USA*, 96, 3396-3403, 1999.
23. Pandolfi M., Amodeo A., Mona L., Pappalardo G., Lidar measurements of aerosol, water vapour and clouds, *Recent Research Developments in Optics*, edited by S.G. Pandalai, Transworld Res. Network, Trivandrum, India, 2003.